

2008, Volume 112C

Chan-Hoe Yip, Yet-Ming Chiang, and Chee-Cheong Wong*:
Dielectric Band Edge Enhancement of Energy Conversion
Efficiency in Photonic Crystal Dye-Sensitized Solar Cell

Page 8735. In our prior work,¹ we presented a schematic of the angular irradiance experiment for the TiO₂ film-photonic crystal (PC) bilayer dye-sensitized solar cell (DSC) (Figure 3b of ref 1). The change in the refracted angle in the

glass substrate of DSC was overlooked and the correction presented here does not modify the qualitative conclusion of ref 1.

The schematic setup of Figure 3 in ref 1 is superseded with Figure 1 shown below. In the original paper¹ and in Figure 1 below, the incidence angle θ is reiterated as the incident angle makes on the air-glass interface. In Figure 1b below, the refracted angle changes according to the law of refraction, $n_i \sin \theta_i = n_{i+1} \sin \theta_{i+1}$, at air-glass interface. The refractive index of glass is 1.5 and air has an index of 1. The light path passes through the inhomogeneous layers of fluorine-doped thin oxide (FTO) and mesoporous TiO₂. Also, it reaches the TiO₂ inverse opal layer with an incidence angle θ_1 . As a summary, the angular irradiance experiment for $\theta = 0, 15$, and 30° results in the incidence angle $\theta_1 = 0, 9.93$, and 19.47° , respectively, at the TiO₂ inverse opal. The symbol θ_1 and its interpretation are addition to the prior paper¹ while θ is restricted to the incident angle of the whole dye-sensitized solar cell.

The photonic band diagram of Figure 5 in ref 1 is superseded with Figure 2 shown below. The change in the angles described above was supported by the use of the corrected lattice parameter of the inverse opal for the rest of the analysis. The lattice parameter, a , was obtained incorrectly from the diameter of the polystyrene colloids previously.¹ Inverse opal undergoes shrinkage under calcination² and the face-centered cubic (111) interplanar distance of 195 nm ($d_{111} = (8/3)^{1/2}r$) is obtained correctly from the scanning electron microscopic image of Figure 2b in ref 1. Therefore, a of the inverse opal is computed to be 337 nm ($a = 2\sqrt{2}r$) and the corrected photonic band diagram was computed as shown in Figure 2 below.

The angle-resolved simulation diagram of Figure 6 in ref 1 is superseded with Figure 3 shown below. On the basis of the new d_{111} obtained above, the corrected transmission and

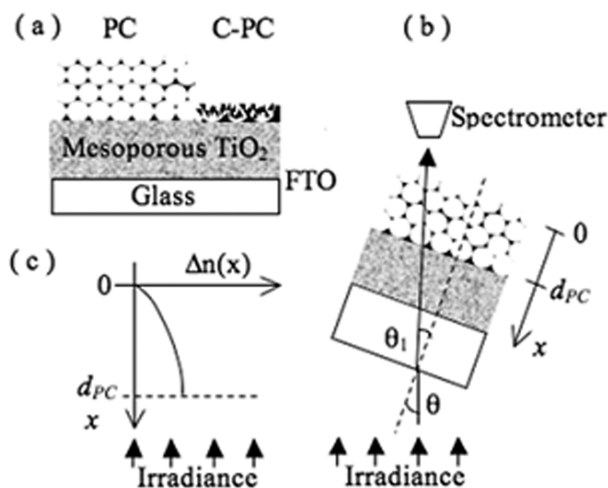


Figure 1. (a) Schematic of a PC and C-PC bilayer electrode on the same FTO substrate. (b) Angular transmission setup for the film-PC bilayer electrode. d_{PC} is the thickness of the PC layer. θ is the incidence angle to the DSC. θ_1 is the refracted angle in the glass substrate and the incident angle to the PC. (c) The expected distribution of the electron injection concentration as the light intensity reduces in the PC.

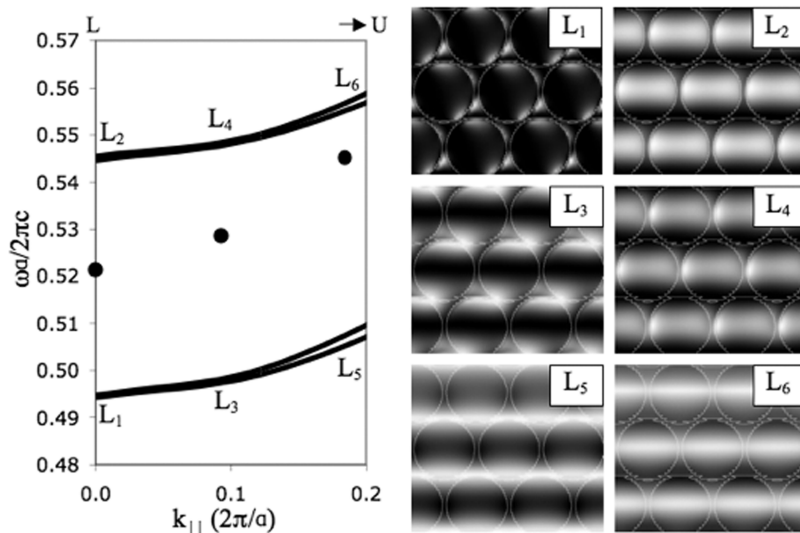


Figure 2. (Left panel) Photonic band diagram of a TiO₂ PC in the LU direction. The y-axis is the angular frequency, ω , normalized with the lattice constant, a , and the speed of light in vacuum, c , and a factor of 2π . The x-axis is the magnitude of the parallel wave vector in the LU direction. L_1 – L_6 denotes the modes at the respective locations in the photonic band diagram. The black dots indicate the transmission dips ($0, 15$, and 30°) in the angle-resolved transmission measurement (from Figure 2). (Right panel) The intensity plot $|E|^2$ of modes L_1 and L_2 (0°), L_3 and L_4 (9.93°), and L_5 and L_6 (19.47°). White indicates high intensity.

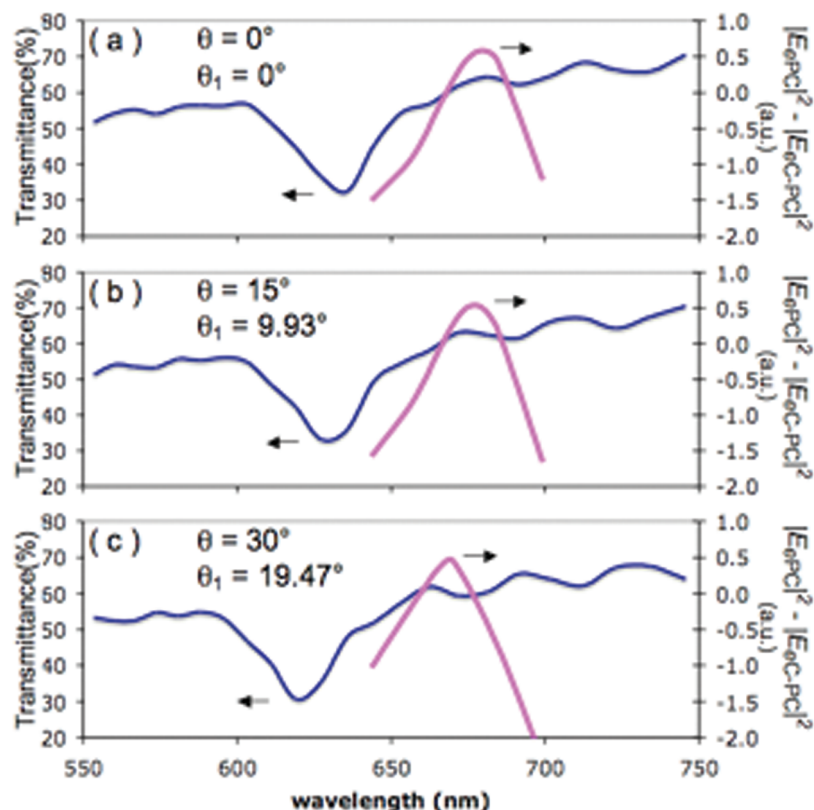


Figure 3. Angled-resolved FDTD simulation of the transmission spectra and time-averaged $|E_{ePC}|^2 - |E_{eC-PC}|^2$ electric field strength plots. The incidence angle (θ_i) at the PC is (a) 0, (b) 9.93, and (c) 19.47° for the angular placement of DSC at 0, 15, and 30°, respectively. The PC enhances electric field strength near the PBG red-edge that shifts in accordance with the PBG.

electric field strength simulations for incidence angle $\theta_i = 0, 9.93$, and 19.47° were plotted in Figure 3a–c. The peak spectral location $|E_{ePC}|^2 - |E_{eC-PC}|^2$ plots in Figure 3 are at 679, 677, and 669 nm for $\theta_i = 0, 9.93$, and 19.47° , respectively, and they blue-shift in accordance with the PBG.

References and Notes

- (1) Yip, C. H.; Chiang, Y. M.; Wong, C. C. *J. Phys. Chem. C* **2008**, *112*, 8735.
- (2) Lee, Y. J.; Braun, P. V. *Adv. Mater.* **2003**, *15*, 563.

10.1021/jp911295c

Published on Web 01/04/2010